

# Statistical Evaluation of Multipath Component Lifetime in the Car-to-Car Channel at Urban Street Intersections Based on Geometrical Tracking

Panagiotis Paschalidis, Kim Mahler, Andreas Kortke, Michael Peter, Wilhelm Keusgen

Fraunhofer Heinrich Hertz Institute  
Einsteinufer 37, 10587 Berlin, Germany  
E-mail: {Panagiotis.Paschalidis}@hhi.fraunhofer.de

**Abstract**—In this paper we present a statistical evaluation of the lifetime of multipath components for the vehicular radio channel. We introduce a new identification and tracking algorithm. The algorithm follows a geometrical approach exploiting the high scatterer resolution in the measurement data and takes as an estimation basis considerations on the relative movement of the scatterer. We sequentially evaluate weighted interrelations between detected contributions in the time-delay domain and decide on common underlying scatterers or not.

We subsequently apply the algorithm to evaluate the measured data. We use wideband channel measurement data collected at urban street intersections under NLOS conditions.

We suggest a classification of distinct and diffuse contributions by means of a threshold with respect to lifetime and discuss on their temporal characteristics, based on an exemplary measurement with typical values. In specific we characterize the lifetime by means of a probability density function and further examine the relation of lifetime and power level of the multipath contribution.

## I. INTRODUCTION

Within the last decade a significant amount of research work has been focused on wireless car-to-car communication systems. A wide range of applications in combination with the promising big deployment potential and expected benefits and profits has led a great deal of public funded as well as automotive industry motivated research in this domain. Research interest in the vehicular channel has risen, when it became clear that off-the-shelf solutions will deliver the expected performance only in the less demanding of the applications and channel conditions. The main advantage of wireless technology over other vehicle-central sensors like radar etc. though come into play in situations where visual contact is limited.

One of the main issues for reliable channel modeling in the vehicular environment in contrast with traditional cellular channel models is the non-stationary character of the channel. The vehicular channel investigation is similar with time series characterization. Stationarity is only given for a short time interval. This has led an increasing number of working groups to adopt geometrical-based non-stationary models in order to elude the stationarity condition for statistical channel modeling but also to offer more accurate models e.g. [1], [2]. Further non-stationary channel models are provided by [3],

who employ a Markov chain to model the birth-death process of the contribution of specific scatterers.

The violation of the stationarity condition is caused by two factors. Through the movement of vehicles the scattering environment changes very quickly, in fact the central moments of the channel characteristic functions can not be reasonably defined over a long period of time. Furthermore significant scatterers are moving in the delay domain (the propagation path becomes longer or shorter). A correlation of neighbouring delay bins is caused, breaching so the uncorrelated scattering condition.

### A. Contribution

The vehicular channel can be characterized by a number of significant scatterer contributions, coming from mostly identifiable scatterers (vehicles, traffic signs, buildings) and a diffuse part. In this paper we introduce an identification and tracking algorithm that can identify the strong multipath contributions. We use measurement data collected in a series of measurement campaigns in order to investigate the lifetime and the power statistics of the stronger scattering contributions, that play a decisive role for the stationarity of the channel. We provide statistics for the urban intersection environment, that can be used for more reliable channel modeling, either for non-stationary geometrical models or for models based on statistical characterization by deducing on stationarity intervals. The scattering contributions are identified in the delay domain and their temporal evolution is tracked in the time domain based on geometrical considerations of the scatterer movement.

### B. Related Work

Previous related work on tracking and lifetime of the scattering contributions was presented in [2]. In that work, a time-delay domain approach is used, using the Hough algorithm to detect slopes. Our work deviates from the Hough algorithm since we found the scatterers to follow additional patterns in the time-delay domain. Furthermore the computational complexity of the algorithm scales unfavorably for dense and noisy matrices (noise or diffuse scattering increases the complexity decisively). In [1], a serial search and subtract

algorithm similar to the CLEAN algorithm and a local linear regression to detect multipath components over time is used.

The question of significant contributions is treated in [4] which presents cluster characterization for the vehicular channel, using the local scattering function (LSF) in order to identify the clusters. Since the LSF is based on the stationarity assumption (locally in time and frequency), a temporal evolution of the LSF (for a given bandwidth) has to be provided. In this work we decided to use the time-delay domain since the high temporal resolution of the measurements provide a very accurate temporal localization and separation of the scatterers.

## II. MULTIPATH COMPONENT TRACKING

The identification of the multipath components in the wide-band channel and the tracking of their temporal evolution is based on the assumption that a single dominant scatterer is behind a strong contribution. This assumption is increasingly valid with increasing resolution in the vehicular channel. Two main characteristics that support this assumption are the outdoor character of the vehicular environment and the relatively small wavelength of the used frequency band. The spatial separation of most important scatterers allows often the identification of their contribution. Indeed the movement of the reflecting physical objects is rather distinct in the impulse response in the form of strong contributions and thus can be tracked in time. In the case of larger structures and surfaces, clusters of contributions are created that have a common behaviour and characteristics, as also noted by e.g. [4].

Relatively simple geometric equations can be used to estimate the temporal evolution of the contribution in the delay domain within a relatively narrow time window where acceleration and speed remain constant. The tracking algorithm is based on the estimation of the temporal evolution in the time-delay domain by means of these geometrical equations. For example, a line in the impulse response is equivalent with a constantly decreasing or increasing propagation distance. Within a small time window most lines can be approximated by linear regressions, a fact also used in [1]. As the time window becomes larger, additional and more accurate estimations can be derived when using polynomials of higher orders.

### A. Measurement Data, Noise, Preprocessing

The measurement data that is used in this investigation was collected in typical urban street intersections; [5] presents and describes one of the campaigns. The measurements stretch over several seconds under NLOS conditions. An important effect connected with long durations in the vehicular environment is the significant power variation, which also affects the noise level. Determining an appropriate noise threshold affects decisively the quality of the results.

We use a double noise threshold in order to account for the fluctuations of the noise level as well as to discard components that are of less importance for the channel. First, we use a threshold relative to the power level of the strongest path component (20 dB lower). This threshold dominates in cases of high SNR; it filters less relevant components. Further, we assume zero mean Gaussian noise and estimate the mean value and variance from the last samples of each impulse

response. Consecutively we set the threshold at four times the standard deviation of the estimated curve. We deferred from a more aggressive threshold (more than four times the standard deviation) in order not to eliminate weak multipath components. This threshold is valid in cases of low SNR, where the channel has weak components.

The measurement data has a multipath delay resolution of 1 ns provided by the bandwidth of the channel sounder used. The high resolution leads to the observation of a large number of distinct multipath components, which is desired since small-scale fading is less pronounced. On the other hand, in the case of a cluster, there is a significant number of neighbouring contributions that distract the algorithm and can be a source of deviation in tracking. Furthermore, uneven surfaces and other unwanted effects can lead to a jitter of the multipath component in the delay domain and disturb the pattern-recognition techniques.

In order to circumvent this difficulty, we decrease the resolution (without inducing fading) of the impulse response  $h$  by filtering  $|h|^2$  with a Gaussian filter. In doing so, we can perform a tracking of the entire cluster of components, which do not drift apart, given the assumption that they are caused mainly by a single physical object. After noise thresholding and filtering we apply peak detection with respect to the delay time in each time sample of the impulse response.

### B. Tracking Algorithm

The identified peaks are evaluated and interrelations are created by weighting the distance of different peaks in terms of delay, power level and time. In this context paths are multipath components that are connected over time. Within the context of the algorithm we name *peak* a local maximum (with respect to the delay time  $\tau$ ) of the channel impulse response. A peak is the contribution of a scatterer for a certain time instant  $t$ . A *path* will denote the (estimated) contribution of a scatterer over time and delay. Consequently, a path can be seen as the temporal evolution of peaks caused by one scatterer.

The main task of the algorithm is to estimate iteratively whether a peak is part of an already identified path or not. Each identified path calculates an estimation of the location of the next peak in time and delay. Then, in consecutive time instants (samples), each new peak evaluates by means of a weight-function and appropriate thresholding the distance from existing estimations, or in other words if it is part of an already identified path. If not, it becomes a new path and enters the pool of identified paths. This is done sequentially for all peaks.

## NOTATION

In outlining the algorithm we will use the following notation and definitions:

- $t_i$ ,  $i = 1 \dots N_t$  and  $\tau_j$ ,  $j = 1 \dots N_\tau$  denote the  $i^{\text{th}}$  time and  $j^{\text{th}}$  delay sample respectively of the sampled time variant impulse response  $h$ . Further we define  $h(t_i, \tau_j) := h_{i,j}$ .
- peak  $m_{i,j}$  is a local maximum of the impulse response with respect to the delay time and is characterized with the triplet  $\{t_i, \tau_j, h_{i,j}\}$ . Where appropriate, we use the

notation  $m_n$  for the  $n^{\text{th}}$  peak, with  $n = 1 \dots N_{\text{peaks}}$ , and  $N_{\text{peaks}}$  the total number of peaks.

- path  $p_k$ ,  $k = 1 \dots N_{\text{paths}}$  is understood as an interrelated set of peaks:  $p_k = \{m_1^k, m_2^k, m_3^k, \dots, m_{N_{\text{peaks}}}^k\}$  with  $m_n^k$  the  $n^{\text{th}}$  peak of a path. The peaks of a path are ordered by time, so  $m_{N_{\text{peaks}}}^k$  is the last peak of  $p_k$ .
- prediction  $\hat{m}^k := \{\hat{t}_i, \hat{\tau}_j, \hat{h}_{i,j}\}$  is the estimated next peak for  $p_k$ . The estimation for  $\hat{t}_i$  and  $\hat{\tau}_j$  is derived by estimating a polynomial up to the second order based on the previous locations of  $p_k$ . The polynomial accounts for differences in relative speed and acceleration of transmitter-receiver and scatterer.
- distance  $d(\hat{m}^k, m_{i,j})$  between prediction  $\hat{m}^k$  and peak  $m_{i,j}$  is defined as  $\{|\hat{t}_i - t_i|, |\hat{\tau}_j - \tau_j|, \hat{h}_{i,j}/h_{i,j}\}$ .

#### ALGORITHM

The initial step of the algorithm is preprocessing of the measurement data which is comprised by noise thresholding and filtering. The further part of the algorithm has three steps:

- Step 1:** Detect and store all peaks  $m_{N_{\text{peaks}}}$  of the time variant impulse response.
- Step 2:** For the current time  $t_i$  (starting from  $t_i = 1$ ) we consider the peaks  $m_{i,1 \dots N_{\text{paths}}}$  and predictions  $\hat{m}^{1 \dots N_{\text{paths}}}$ . For each peak  $m_n$  evaluate the distance  $d(\hat{m}^k, m_n)$  for all existing paths  $p_{1 \dots N_{\text{paths}}}$ :  
If  $d(\hat{m}^k, m_n) < d_{\text{max}}$  then store  $p_k$  as a path-candidate for  $m_n$ . Each candidate is assigned a weight  $W_{k,n} = f(d(\hat{m}^k, m_n))$ . A threshold discards all path-candidates with  $W_{k,n} < W_{\text{min}}$ . If the evaluation returns no path-candidates for a peak, a new path is created starting from the current peak.  
In other words, this step practically evaluates the prediction of all existing paths and assigns to each of the peaks (in a time instant) a list of valid path-candidates with their corresponding weight factor.
- Step 3:** Sort and select the path-candidates for each peak so that the aggregate  $W_{k,n}$  for all peaks of a time instant is jointly maximized. Paths with predictions further than a threshold time distance  $d_{\text{max}}$  are removed from the search pool. Return to Step 2 if  $t_i < t_{N_t}$ .

In the end of these steps, we have a list of all paths up to the final time instant  $t_{N_t}$ . In the final stage, we use the impulse response with the full bandwidth to pinpoint the dominant contributions and analyse the results.

#### C. Distance-weight Function

A crucial element of the algorithm is the weight function, that prioritizes the path-candidates according to their prediction for a given peak. The distance-weight function  $f(d(\hat{m}^k, m_n))$  is displayed in Fig. 1 and was created based on the following considerations.

In the delay domain, we assume that our estimation is normally distributed around the real value. The assumption is based on jitter and noise considerations. In the time domain, we assume that the probability, of a path appearing after  $dt$  time samples without intermediate peaks decays exponentially from the last time sample of the path. For both domains

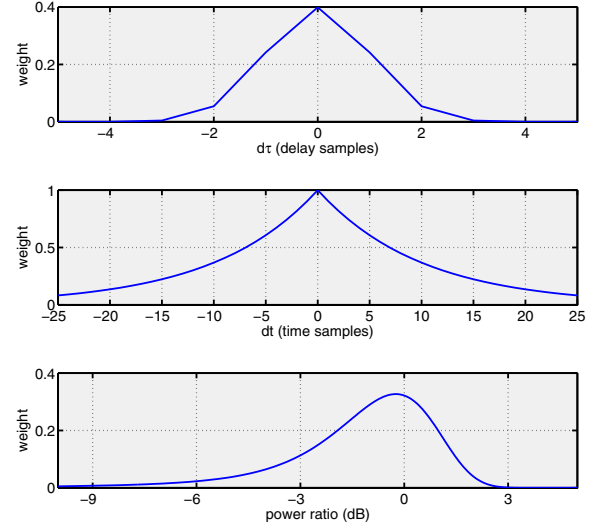


Fig. 1. Distance-weight function  $f(d(\hat{m}^k, m_n))$ .

we used sampled versions of the corresponding PDFs. With respect to the power, we assume approximately rician fading and weight the amplitude ratio with a rician distribution. Since we found the power ratio to be more important on the validity of the decision, the power ratio weight is higher. Finally, we assign a confidence factor for paths with many samples.

It should be noted that the weight function, although sourced on theoretical considerations, it does not fulfill the requirements of a PDF nor is it intended to do so. It is a relative comparison measure with other path-candidates rather than an absolute probability (density) function. The values for the function were derived iteratively, by visual inspection of the results of the algorithm and validation with measurement data.

#### D. Considerations on the Algorithm

The algorithm returns very satisfying results for path detection and tracking. Nevertheless it is also subject to certain limitations that influence the results. One of the most important limitations is the sequential processing. Sequential processing implies that the decision at each point is made only by considering information of the past, thus with limited information compared to the full impulse response information. This renders the algorithm less robust to decision errors and error propagation with little chance to recover a posteriori in the event of a deviation. An other decisive challenge is the proper parametrization of the weight function. A trade-off has to be met which will neither create non-existing or non-intuitive paths, but also will not oversee important paths on the other hand. In fact the inherent properties of the vehicular channel set strong challenges for the parametrization. The fast and strong fluctuations that limit the temporal validity of statistically derived values, or in the best case introduce very strong variances, increase the probability of errors in tracking.

### III. RESULTS

#### A. Lifetime of Distinct and Diffuse Components

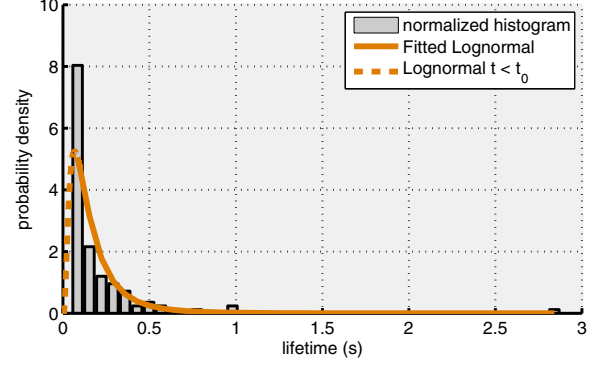
In the following, we will use an exemplary measurement to portray typical results. The initial impulse response of the measurement is shown in Fig. 3(a).

The algorithm sets initially no limitations on the lifetime of a path, implying that a path can also contain only a single peak. Since we have used a conservative noise threshold in the beginning, we have decided to discard all paths with a single peak in order to eliminate noise contributions.

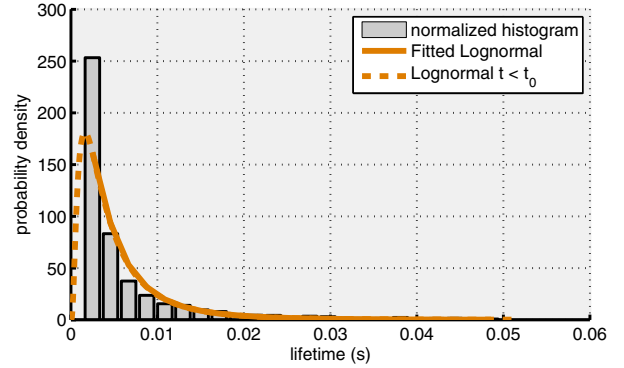
We then investigated the lifetime distribution of the detected paths. Since we assume the lifetime of a path being a continuous process we need a density function over the continuous random variable lifetime  $X_L$ . For that we examined the normalized histogram (density), which is given by the count of occurrences, normalized by the total number of the events and the bin width. We have found that the lifetime distribution of all paths is approximated best when we divide the set of the paths into two categories. The first category are very dense, short-lived contributions while the second is rare but long-lived contributions. Both sets can be fitted with a lognormal distribution. The appropriate threshold with respect to lifetime was found to be at 50 ms. In Figures 2(a) and 2(b) we display the fitted distributions derived from the measurement data in Fig. 3(a), for paths with lifetime bigger and smaller than the threshold of  $T_L = 50$  ms respectively. The values for the distributions are  $\{\mu_{X_L \geq T_L}, \sigma_{X_L \geq T_L}\} = \{-2.036, 0.806\}$  and  $\{\mu_{X_L < T_L}, \sigma_{X_L < T_L}\} = \{-5.608, 0.904\}$ .

If we consider the sampling interval for this measurement being at approx. 700  $\mu$ s and the relatively low speeds of the vehicles in urban environments, we can assume that paths resulting from single reflecting objects must have a minimum lifetime. Paths with shorter lifetime can be the result of different effects like small-scale fading and diffuse scattering. In these cases, the nature of the scatterer or a clear structure in the time-delay evolution cannot be identified. As noted in [6], diffuse scattering has a rather simple structure in the Doppler delay domain. Nevertheless, diffuse scattering has been identified to carry an important part of the channel power. E.g. [7] is suggesting a computationally efficient model, complementing the modeling approach used in [1]. We will use the threshold  $T_L$  in order to distinguish between distinct and diffuse (or other short-lived) path components.

Figure 3(b) displays the detected distinct paths next to the measured impulse response (Fig. 3(a)). The algorithm fares well, considering the low SNR especially in the first seconds and the dense multipath channel. The measurement targets a typical NLOS, intersection radio channel. Until approx. the sixth second, the strongest contribution lies at approx. half of the excess delay, surrounded by often very weak contributions. The most pronounced ones are tracked by the algorithm, as also the strongest contribution. Typical for urban intersections, as long as the vehicles are deep in the building canyons, most contributions are parallel to each other suggesting that they come from static scatterers, probably buildings or other good scattering objects on the intersection. Note the high resolution and the accuracy in tracking in Fig. 3(b).



(a) Paths with lifetime  $X_L \geq T_L$



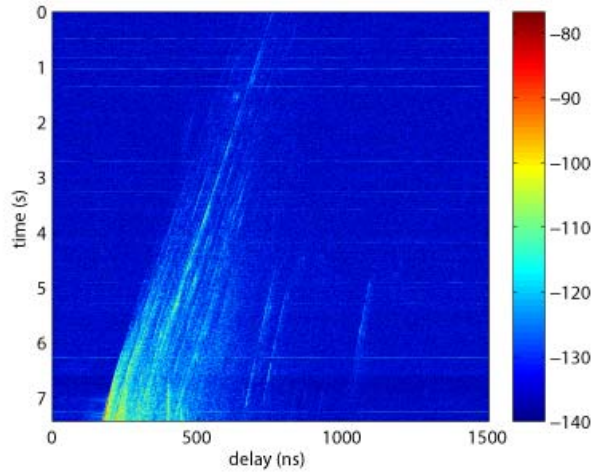
(b) Paths with lifetime  $X_L < T_L$

Fig. 2. Path detection on an exemplary impulse response.

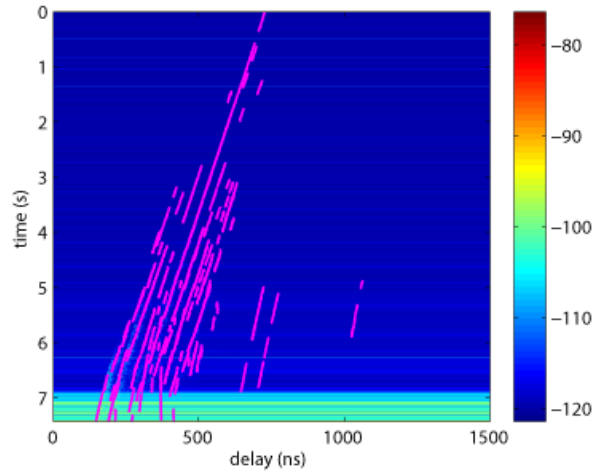
#### B. Relation of Lifetime with Power

Finally we investigated the relation of path lifetime with relative power level. Figure 4 depicts all detected paths with respect to their lifetime and the relative mean power. A blue circle denotes the mean power of a path with lifetime less than  $T_L$ , while a red cross indicates a path with lifetime over the threshold  $T_L$ . Intuitively, strong contributions come mostly from reflecting objects in the vicinity of the transmitter or the receiver. Given the mobility of the scatterers, if we consider shadowing as a main reason for the disappearing of a path, then it is less likely for other objects to interfere or to obstruct the propagation path when the proximity of a scatterer to the transmitter or the receiver increases. Following this consideration, strong scatterers should have in general longer life. On the contrary, it is less likely for scatterers that lie further to maintain an unobstructed propagation path for a longer time. Thus, weaker paths are expected to be more short-lived.

This line of thought is partly validated by Fig. 4. If we examine the relation between path density, power level and lifetime, we observe that while for short lifetimes, the vast majority of paths are low-powered, as the lifetime increases, the detected paths become more equally distributed over the power levels. The effect is more pronounced if we consider the following classification issues: during the approx. 7.4 s of the measurement, the channel fluctuates over 40 dB. Paths with longer lifetime will most probably suffer from similarly strong



(a) Channel impulse response



(b) Detected paths on channel impulse response

Fig. 3. Path detection algorithm applied on an exemplary channel impulse response.

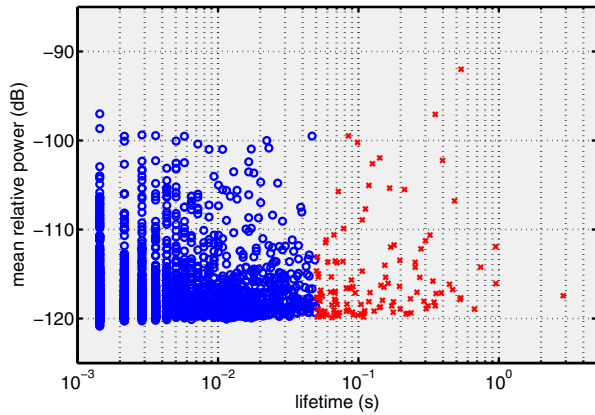


Fig. 4. Mean relative power level of a path over lifetime.

fluctuations which decrease the mean. Furthermore, sometimes, the strong fluctuations or longer shadowing intervals cause the algorithm to result in two different paths for each part of the path. This effect results in classifying a longer path as two shorter-lived (but still with high power).

#### IV. CONCLUSION

In this paper, we have investigated the lifetime of multipath contributions of the vehicular channel for urban intersections under NLOS conditions, with the use of wideband measurement data. In order to identify the contributions and assess their lifetime, we introduced a new geometrically motivated path tracking algorithm, which was applied on the appropriately preprocessed channel impulse response. The algorithm was parametrized and trained on the existing measurement data. After inspection of the results, the detection and the tracking provide a fairly congruent result with human intuition, nevertheless one must be aware of its limitations. Subsequently, we use an exemplary measurement to provide typical results about the lifetime, also investigating the inter-

dependency with power. We have derived a threshold with respect to lifetime to separate distinct multipath components that follow a structured course in the time delay domain and have a minimum lifetime from diffuse ones that are mostly short lived. The evaluation of the statistics resulted in a good fit for lognormal distributions for each of the different types of contributions validating the separation of the two types.

#### ACKNOWLEDGEMENT

This work results from the joint project Ko-KOMP, which is part of the project initiative Ko-FAS, and has been funded by the German Bundesministerium für Wirtschaft und Technologie (Federal Department of Commerce and Technology) under grant number BMWi 19S9024E.

#### REFERENCES

- [1] J. Karedal, F. Tufvesson, N. Czink, A. Paier, C. Dumard, T. Zemen, C. Mecklenbrauker, and A. Molisch, "A geometry-based stochastic mimo model for vehicle-to-vehicle communications," *Wireless Communications, IEEE Transactions on*, vol. 8, no. 7, pp. 3646–3657, 2009.
- [2] O. Renaudin, V. Kolmonen, P. Vainikainen, and C. Oestges, "Car-to-car channel models based on wideband MIMO measurements at 5.3 GHz," in *Conference on Antennas and Propagation, 2009. EuCAP2009-Spring. 2009 IEEE 3rd*, 2009.
- [3] I. Sen and D. Matolak, "Vehicle-vehicle channel models for the 5 GHz band," *Intelligent Transportation Systems, IEEE Transactions on*, vol. 9, no. 2, pp. 235–245, 2008.
- [4] L. Bernadó, A. Roma, N. Czink, A. Paier, and T. Zemen, "Cluster-based scatterer identification and characterization in vehicular channels," in *Wireless Conference 2011 - Sustainable Wireless Technologies (European Wireless), 11th European*, 2011, pp. 1–6.
- [5] P. Paschalidis, K. Mahler, A. Kortke, M. Peter, and W. Keusgen, "2 x 2 MIMO measurements of the wideband car-to-car channel at 5.7 GHz on urban street intersections," in *Vehicular Technology Conference (VTC Spring), 2011 IEEE 74th*, 2011, pp. 1–5.
- [6] P. Paschalidis, K. Mahler, A. Kortke, M. Peter, M. Wisotzki, and W. Keusgen, "Statistical evaluation and modeling of the wideband car-to-car channel at 5.7 GHz," in *Electromagnetic Theory (EMTS), 2010 URSI International Symposium on*, 2010, pp. 876–879.
- [7] N. Czink, F. Kaltenberger, Y. Zhou, L. Bernadó, T. Zemen, and X. Yin, "Low-complexity geometry-based modeling of diffuse scattering," in *Antennas and Propagation (EuCAP), 2010 Proceedings of the Fourth European Conference on*, 2010, pp. 1–4.